

See discussions, stats, and author profiles for this publication at: <https://www.researchgate.net/publication/224538453>

# „Thermal Ignition of Explosives”

ARTICLE *in* JOURNAL OF APPLIED PHYSICS · MARCH 1960

Impact Factor: 2.18 · DOI: 10.1063/1.1735565 · Source: IEEE Xplore

---

CITATIONS

100

---

READS

52

2 AUTHORS, INCLUDING:



Charles Mader

Mader Consulting Co.

189 PUBLICATIONS 1,310 CITATIONS

SEE PROFILE

## Thermal Initiation of Explosives

John Zinn and Charles L. Mader

Citation: *J. Appl. Phys.* **31**, 323 (1960); doi: 10.1063/1.1735565

View online: <http://dx.doi.org/10.1063/1.1735565>

View Table of Contents: <http://jap.aip.org/resource/1/JAPIAU/v31/i2>

Published by the [American Institute of Physics](#).

---

### Additional information on J. Appl. Phys.


Journal Homepage: <http://jap.aip.org/>

Journal Information: [http://jap.aip.org/about/about\\_the\\_journal](http://jap.aip.org/about/about_the_journal)

Top downloads: [http://jap.aip.org/features/most\\_downloaded](http://jap.aip.org/features/most_downloaded)

Information for Authors: <http://jap.aip.org/authors>

## ADVERTISEMENT



**AIPAdvances**

Special Topic Section:  
**PHYSICS OF CANCER**

Why cancer? Why physics?

[View Articles Now](#)

## Thermal Initiation of Explosives

JOHN ZINN AND CHARLES L. MADER\*

*University of California, Los Alamos Scientific Laboratory, Los Alamos, New Mexico*

(Received July 29, 1959)

Numerical solutions have been obtained for the nonlinear heat conduction equations arising in the theory of thermal explosions. Explosion times are calculated for externally heated spheres, cylinders, and slabs of several explosive materials, and the results are shown to agree with experiment.

### INTRODUCTION

IF an explosive is heated or cooled, and if it decomposes according to a single first-order rate process, its internal temperature should be described by the equation,<sup>1</sup>

$$-\lambda \nabla^2 T + \rho C (\partial T / \partial t) = \rho Q Z e^{-E/RT}. \quad (1)$$

Here  $T$  is temperature in  $^{\circ}\text{K}$ ,  $\lambda$  is thermal conductivity ( $\text{cal deg}^{-1} \text{cm}^{-1} \text{sec}^{-1}$ ),  $\rho$  is density ( $\text{g cm}^{-3}$ ),  $C$  is heat capacity ( $\text{cal g}^{-1} \text{deg}^{-1}$ ),  $Q$  is heat of decomposition ( $\text{cal g}^{-1}$ ),  $Z$  is collision number ( $\text{sec}^{-1}$ ),  $E$  is activation energy ( $\text{cal M}^{-1}$ ),  $R$  is the gas constant ( $1.987 \text{ cal M}^{-1} \text{deg}^{-1}$ ).

It will be assumed that the above constants are independent of temperature.

The Laplacian operator  $\nabla^2$ , in the special cases of spheres, infinitely long cylinders, or infinite slabs, reduces to

$$(\partial^2 / \partial x^2) + (m \partial / x \partial x),$$

if we require that the heating be uniform over the surface, ( $m=0$  for slabs, 1 for cylinders, and 2 for spheres).

Where the reaction-heating term  $(\rho Q Z) \exp(-E/RT)$  is zero, Eq. (1) reduces to the well-known heat equation. In the one-dimensional case (infinite slab) this is

$$\partial^2 T / \partial x^2 = \rho C \partial T / \lambda \partial t. \quad (2)$$

Under the boundary conditions  $T = f_0(x)$ , when  $t=0$  and  $T = T_1$  at  $x=0$  and  $x=2a$ , Eq. (2) has the solution:

$$T(x,t) = T_1 + \sum_{n=1}^{\infty} \exp\left(-\frac{n^2 \pi^2 \lambda t}{4 \rho C a^2}\right) \times \sin \frac{n \pi x}{2a} \int_0^{2a} [f_0(x) - T_1] \sin \frac{n \pi x}{2a} dx. \quad (3)$$

If at any time the temperature  $f_0(x)$  is known at a sufficient number of points, the integrals can be evaluated numerically; thus the temperature distribution at later times can be calculated.

When the self-heating term is nonzero, we have for the infinite slab,

$$-\lambda (\partial^2 T / \partial x^2) + \rho C (\partial T / \partial t) = \rho Q Z e^{-E/RT},$$

which has not been solved analytically. However, numerical solutions can be obtained in the following manner.

Suppose the time scale to be divided into equal intervals each  $\tau$  sec long. We imagine that the heat of reaction is not liberated continuously, but instead is added to the system batchwise at the end of each interval. For purposes of calculating the amount of reaction heat liberated at any point in an interval  $\tau$  it is convenient to assume that the temperature remains constant during  $\tau$ , an approximation which improves as the intervals are made shorter. Thus, if in the absence of reaction during  $\tau$  we calculate that the temperature at some point should be  $T$ , we can estimate that the reaction that has occurred in the interval should actually raise the temperature at the point to  $T + (QZ\tau/C) \exp(-E/RT)$ .

Suppose the slab is initially at a uniform low temperature  $T_0$ . At time zero the two faces at  $x=0$  and  $x=2a$  are suddenly raised to a higher temperature  $T_1$ . Treating the problem for the first small interval  $\tau_1$  as though the slab were inert, we obtain an approximation to the temperature distribution  $T(x, \tau_1)$  after  $\tau_1$  sec, as given by Eq. (3), where  $f_0(x)$  is set equal to  $T_0$  and  $t = \tau_1$ . Due to the chemical reaction which will have occurred, this first estimate of the temperature should be revised to  $T(x, \tau_1) + (QZ\tau_1/C) \exp[-E/RT(x, \tau_1)]$ . During the next interval  $\tau_2$  the slab is again treated as inert, and a first approximation to the temperature is again given by Eq. (3), where this time we must set  $f_0(x)$  equal to  $T(x, \tau_1) + (QZ\tau_1/C) \exp[-E/RT(x, \tau_1)]$ , and  $t$  equal to  $\tau_2$ . Again the temperature rise due to reaction is added on. This process is repeated either until a steady state is attained, or until the temperature at some point in the slab reaches some very high value which may be said to define an explosion.

An exactly analogous technique has been applied to cylinders, where the inert heat equation takes the form,

$$\partial^2 T / \partial r^2 + (\partial T / r \partial r) = \rho C \partial T / \lambda \partial t.$$

Under the boundary conditions  $T = f_0(r)$  when  $t=0$  and

\* Work performed under the auspices of the U. S. Atomic Energy Commission.

<sup>1</sup> D. A. Frank-Kamenetskii, *Acta Physiochim. U.R.S.S.* **10**, 365 (1939).

$T = T_1$  for  $r = a$ , this has the solution

$$T(r,t) = T_1 + \frac{2}{a^2} \sum_{n=1}^{\infty} \frac{\exp[-(g_n^2 \lambda t / \rho C a^2)]}{J_1^2(g_n)} \times J_0\left(\frac{g_n r}{a}\right) \int_0^a r(f_0(r) - T_1) J_0\left(\frac{g_n r}{a}\right) dr, \quad (4)$$

where the  $g_n$  are the roots of the zero-order Bessel function  $J_0$ .

The procedure has also been applied to spheres. Here the inert heat equation is

$$\partial^2 T / \partial r^2 + 2\partial T / r \partial r = \rho C \partial T / \lambda \partial t,$$

and under the boundary conditions  $T = f_0(r)$  when  $t = 0$  and  $T = T_1$  for  $r = a$  this has the solution:

$$T(r,t) = T_1 + \frac{2}{ar} \sum_{n=1}^{\infty} \exp\left(-\frac{n^2 \pi^2 \lambda t}{\rho C a^2}\right) \times \sin \frac{n \pi r}{a} \int_0^a r(f_0(r) - T_1) \sin \frac{n \pi r}{a} dr. \quad (5)$$

The calculations were carried out on an IBM-704 digital computer.

## RESULTS—GENERAL

The gross results of the calculations are not at all unexpected and might be summarized as follows.

If a given explosive in a charge of a given size and shape has its surface maintained at a temperature higher than a certain critical value, which we designate by  $T_m$ , it will eventually explode. If the surface temperature is kept below  $T_m$  a thermal explosion will not occur. This critical temperature decreases as the dimensions of the charge are increased.

If the charge is initially at room temperature, and its surface temperature is then raised to  $T_1$ , where  $T_1$  is above  $T_m$ , the explosion will occur after a certain

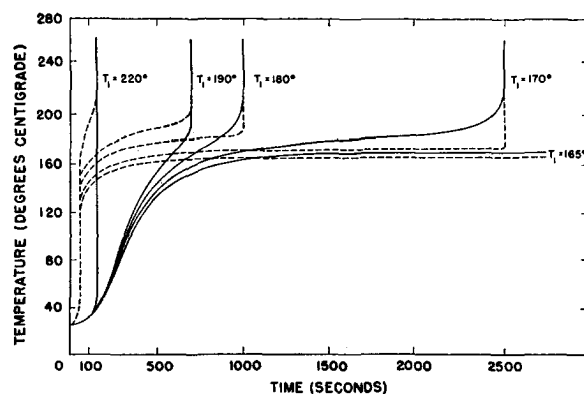


FIG. 1. Temperature vs time at two locations within a 1 in. diam sphere of RDX initially at 25°C for various values of  $T_1$ . Solid curve:  $r/a = 0$  (center of sphere); Dashed curve:  $r/a = 0.9$ .

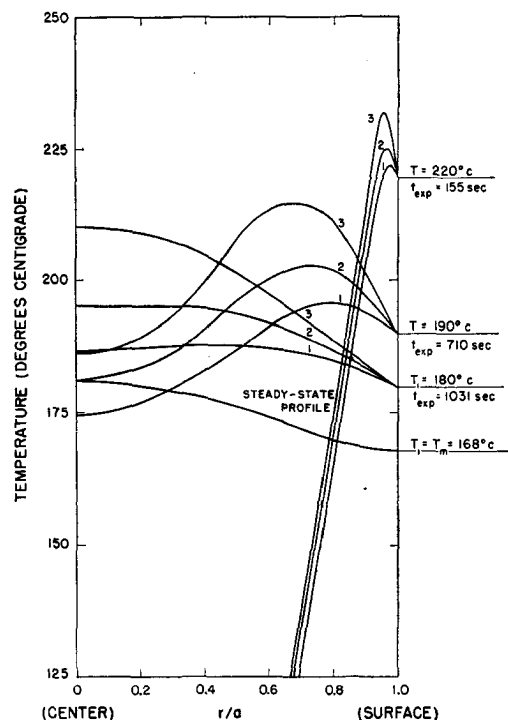


FIG. 2. Temperature profiles for times near the end of the induction period, as calculated for 1 in. spheres of RDX initially at 25°C. Curve 1:  $t = 0.90 t_{exp}$ ; Curve 2:  $t = 0.95 t_{exp}$ ; Curve 3:  $t = 0.98 t_{exp}$ . Also shown is the steady-state profile at the critical temperature,  $T_m$ .

induction time which depends on the explosive, the geometry of the charge, and  $T_1$ . If  $T_1$  is only slightly higher than the critical temperature  $T_m$  the induction time is relatively long, and the explosion develops at the center of the charge. With increasingly higher values of  $T_1$  the induction time becomes progressively shorter and the explosion commences progressively closer to the surface. (See Figs. 1 and 2.) For a given value of  $T_1$  the induction times for small charges are much shorter than for large ones.

Figure 1 shows the calculated variation of temperature with time at two locations within a 1-in. sphere of RDX for various values of  $T_1$ . For relatively low surface temperatures the hottest region prior to explosion is at the center. Points near the surface remain relatively cool until the end of the induction period, suffering a discontinuous jump at the time of explosion. Somewhat the reverse situation applies when  $T_1$  is high. The same facts are evident from Fig. 2, where the temperature vs position profiles are shown for various times near the end of the induction period.

For charges of a given size, shape, and composition it is convenient to plot logarithms of the calculated explosion times vs the reciprocal of the surface temperature  $T_1$ , where the charges all start out at a uniform low temperature  $T_0$ . For slabs, cylinders, and spheres these plots are linear over quite a large region, but bend upward sharply near the critical temperature  $T_m$ . At  $T_m$

they become vertical, indicating an infinitely long induction period.

Frank-Kamenetskii<sup>1</sup> and Chambré<sup>2</sup> have solved Eq. (1) under the steady state condition  $\partial T/\partial t = 0$ , obtaining the following expression for critical temperature in terms of the related physical parameters:

$$T_m = \frac{E}{2.303R \log(\rho a^2 QZ E / \lambda R T_m^2 \delta)}, \quad (6)$$

where  $\delta = 0.88$  for slabs, 2.00 for cylinders, and 3.32 for spheres. This equation can be quickly solved by iteration and gives values for  $T_m$  which are in agreement with those obtained from the present calculated  $\log t_{\text{exp}}$  vs  $1/T_1$  curves.

It will be noted from the method of calculation and from the form of Eqs. (3)–(5) that for a given shape only three parameters are used to describe the charge, namely  $\rho a^2 QZ/\lambda$ ,  $E$ , and  $\lambda/\rho C a^2$ , instead of seven independent ones. Thus one can make the following generalizations: (1) Changing  $Q$  by a multiplicative factor is entirely equivalent to changing  $Z$ ; (2) In the same way,  $\rho$ ,  $a^2$ , and  $1/\lambda$  are equivalent; (3)  $E$  and  $C$  are independent of the others.

The  $t_{\text{exp}}$  vs  $1/T_1$  relationship is of the form

$$t_{\text{exp}} = \frac{\rho C a^2}{\lambda} F(E/T_m - E/T_1), \quad (7)$$

where  $F$  is a function depending only on the type of geometry (spheres, cylinders, or slabs) and the initial temperature  $T_0$ . Values of  $F$  as a function of the argument,  $E/T_m - E/T_1$  are plotted in Fig. 3 for spheres, cylinders, and slabs, all initially at 25°C. Since  $T_m$  is given by Eq. (6), the relationship (7) together with Fig. 3 makes possible the calculation of explosion times for spheres, cylinders, or slabs of any arbitrary explosive (when  $\rho$ ,  $C$ ,  $a$ ,  $\lambda$ ,  $Z$ ,  $Q$ , and  $E$  are known).

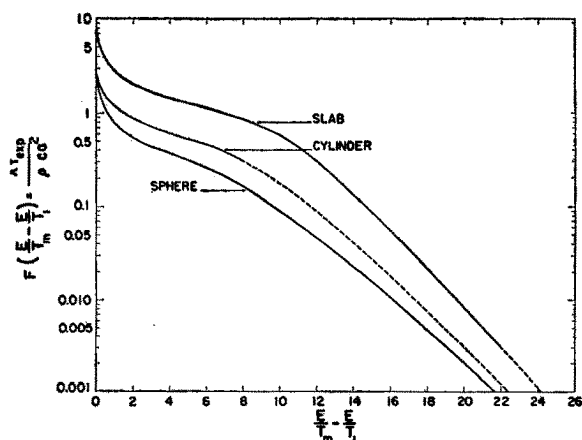


FIG. 3. Graphs of  $\lambda t_{\text{exp}}/\rho C a^2$  vs  $E/T_m - E/T_1$  for spheres, cylinders, and slabs, all initially at 25°C.

<sup>2</sup> P. L. Chambré, J. Chem. Phys. **20**, 1795 (1952).

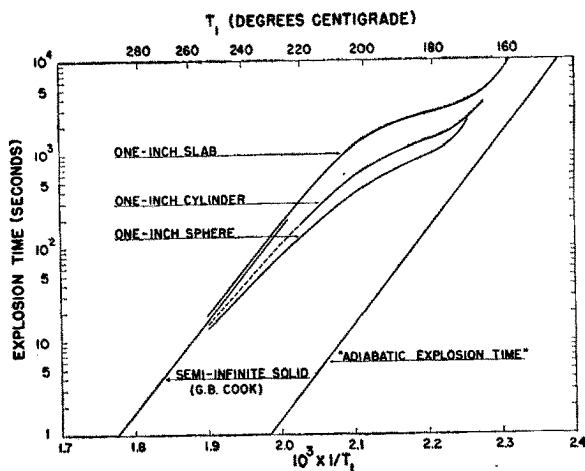


FIG. 4. Explosion times vs  $1/T_1$  for RDX in various geometries. Initial temperature = 25°C.

Figure 4 shows the calculated explosion times vs temperature for three particular cases, namely 1 in. RDX spheres, cylinders, and slabs. The results can be explained qualitatively as follows. The critical temperatures  $T_m$  below which no explosions are obtained are related to the rate at which heat can escape to the surface, which in turn is related to the surface-to-volume ratio. The surface-to-volume ratios of spheres, cylinders, and slabs are respectively  $3/a$ ,  $2/a$ , and  $1/a$ , if  $a$  represents radius or half-thickness. Thus for a given value of  $a$  the slab should have the lowest critical temperature. At relatively low temperatures explosion times are related to surface-to-volume ratios in the opposite manner. The sphere, having the smallest volume to be heated per unit surface, will explode the fastest.

Although at relatively low temperatures geometry has an important influence on induction times, its effect becomes less pronounced as temperature is increased. This is associated with the fact that for high external temperatures explosions begin near the surface of the explosive while the interior is still cool. Above 270°C the  $\log t_{\text{exp}}$  vs  $1/T_1$  plots for 1 in. RDX spheres, cylinders, and slabs are coincident (Fig. 4). Moreover they are coincident with the plots obtained by G. B. Cook<sup>3</sup> for a semi-infinite solid heated at its single surface. Cook's line, adjusted to correspond to our own choice of physical parameters, is included in Fig. 4.

Also plotted in Fig. 4 are "adiabatic" explosion times, defined by the relation

$$t_{\text{exp}} = \int_{T_1}^{T_{\text{exp}}} \frac{C}{QZ} \exp(E/RT) dt \approx \frac{CRT_1^2}{QZE} \exp(E/RT_1).$$

Physically this represents the time it would take for an infinite mass of explosive to ignite if it were initially at the uniform temperature  $T_1$ . The adiabatic explosion

<sup>3</sup> G. B. Cook, Proc. Roy. Soc. (London) **246**, 154 (1958).

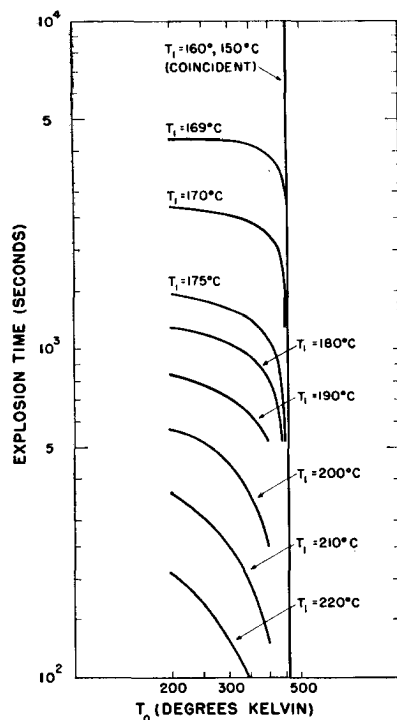


FIG. 5. Explosion time vs initial temperature for 1-in. RDX spheres at various values of  $T_1$ .

time is necessarily shorter than explosion times obtained on raising only the surface of the explosive to  $T_1$ .

The effect of initial temperature on explosion times has been investigated only for the case of spheres. Plots of explosion times for 1 in. RDX spheres vs their initial temperature  $T_0$  are shown in Fig. 5, for various values of the surface temperature  $T_1$ . The following qualitative observations can be made: (1) If the explosive is initially cold, and its surface is raised to a temperature only slightly above  $T_m$ , the precise value of the initial temperature is relatively unimportant. The body of the explosive heats relatively quickly to  $T_1$ , regardless of the initial temperature. Then commences the slow process of self-heating, which takes up the major part of the induction period. For higher values of  $T_1$  this is no longer the case. The self-heating process takes proportionately less time, and it is strongly influenced by conduction of heat to the cold interior; (2) If the initial temperature is less than  $T_1$ , and  $T_1$  is lower than the critical temperature  $T_m$  no thermal explosions can occur. However, if  $T_0$  exceeds  $T_1$  (a rather hypothetical situation), explosions may occur even when the surface temperature is lower than  $T_m$ . For every value of  $T_1$  below  $T_m$  there is a "critical" value of  $T_0$  which, if exceeded, will lead to an explosion. This is related to the matter of "hot spots"<sup>4</sup> and will not be discussed further here.

Corresponding to the reduced explosion time plots of Fig. 3, in Fig. 6 the quantity  $\lambda_{\text{exp}}/\rho Ca^2$  is plotted vs  $E/T_m - E/T_1$  for spheres with various initial tempera-

tures. Figure 6, together with Eqs. (6) and (7), makes possible the calculation of explosion time for any sphere with any value of  $T_0$ .

The present calculational technique is limited in practice to temperatures not too far in excess of  $T_m$ . Within this region the reaction rate term is relatively small; hence the size of the time intervals  $\tau$  can be made large enough to allow the Fourier series in (3), (4), and (5) to converge at a reasonable rate. By varying  $\tau$  it is found that accuracy suffers at temperatures where  $(QZ\tau/C) \exp(-E/RT)$  exceeds  $1^\circ\text{C}$ .

For economy of computing time it has been necessary to write a series of machine programs for each of the geometries considered. To cover a region of temperatures near to or lower than  $T_m$  a program is used which carries the Fourier series summations over sixteen terms and performs integrations by means of Simpson's rule. When more terms are considered Simpson's rule becomes inefficient, and it has been necessary to use a method which is similar in principle to that of Filon<sup>5</sup> although not requiring that the region of integration be divided into equally spaced intervals.<sup>6</sup> The most extensive machine programs extend the Fourier summations over 500 terms, allowing  $\tau$  to be as small as  $5\rho Ca^2/\lambda \times 10^{-6}$ .

#### SPECIFIC CALCULATIONS

Reliable thermochemical data for explosives are quite scarce. Much of the available literature is abstracted in Picatinny Arsenal Report 1740 (1958), and the parameters used in these calculations are mostly from this source. For other parameters where no data exist, one is forced to guess, and the guesses which appear here are probably reliable to within a factor of three.

Literature values for  $E$  and  $Z$  are generally in poor agreement. The uncertainties are of such magnitude as

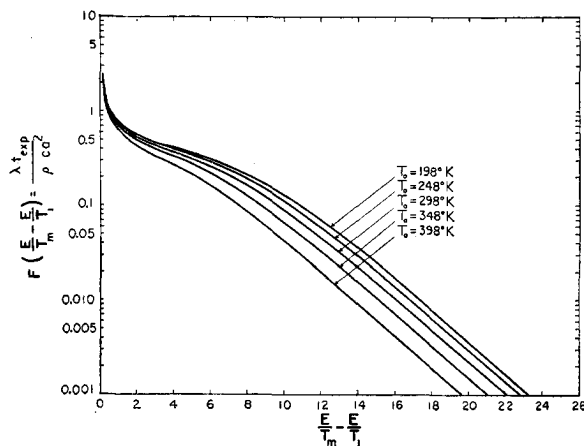


FIG. 6. Graphs of  $\lambda_{\text{exp}}/\rho Ca^2$  vs  $E/T_m - E/T_1$  for spheres with various initial temperatures.

<sup>5</sup> L. N. G. Filon, Proc. Roy. Soc. (Edinburgh) **49**, 38 (1928-1929).

<sup>6</sup> John Zinn, Commun. Assoc. Computing Machinery (to be published).

<sup>4</sup> E. K. Rideal and A. J. B. Robertson, Proc. Roy. Soc. (London) **A195**, 135 (1948).

Table I. Parameters used in the calculations.

Explosive	$\rho$ (g/cc)	$C$ cal/g/°C	$\lambda$ cal/°C/cm/sec	$Q$ cal/g	$Z$ sec <sup>-1</sup>	$E$ kcal/M	Source of $E$ and $Z$
RDX	1.8	0.5	0.0007	500	$10^{18.5}$	47.5	Robertson <sup>8</sup>
75/25 cyclitol	1.7	0.5	0.0007	375	$10^{18.5}$	47.5	Robertson <sup>8</sup>
50/50 pentolite	1.65	0.5	0.0005	250	$10^{23.1}$	52.3	Robertson <sup>9</sup>
TNT	1.6	0.5	0.0005	500	$10^{11.4}$	34.4	Robertson <sup>10</sup>
TNT	1.6	0.5	0.0005	500	$10^{12.2}$	43.4	Cook and Abegg <sup>11</sup>

to overshadow any uncertainties arising from the other parameters. Experiments at this Laboratory<sup>7</sup> tend to confirm the kinetic constants determined by Robertson<sup>8,9</sup> for RDX and PETN, and these were used in the calculations. For TNT, on the other hand, values of  $E$  and  $Z$  were determined both by Robertson<sup>10</sup> and by Cook and Abegg,<sup>11</sup> and their disagreement causes a difference of 90° in  $T_m$  as calculated by Eq. (6).

Data on heats of decomposition are nonexistent. The value of 500 cal/g is assumed here for all explosives considered.

For mixed explosives like pentolite and cyclitol, the induction times are determined almost entirely by the more reactive component. The TNT acts mainly as a diluent, since it does not decompose appreciably below temperatures where self-heating by the other component is extremely fast. Thus for 50/50 pentolite we assume that the activation energy has the value appropriate for PETN (52.3 kcal per M), and the  $QZ$  has one-half the PETN value.

Log  $t_{\text{exp}}$  vs  $1/T_1$  curves have been calculated for 1-in. cylinders of each of the explosives tested in Table I,

using the parameters indicated. The curves are shown in Fig. 7 along with experimental points.

## EXPERIMENTAL

The experiment to be described was not specifically designed to fit the present model. Historically the shots preceded the calculations by a few years. Nevertheless, the resemblance is strong and a comparison of the data with the theory is of interest.

The main difference between the idealized model and "reality" lies in the fact that most explosives melt before much decomposition occurs. In all cases the kinetic parameters used in the calculations were determined above the melting point. However, no attempt has been made to allow for the changes in heat transfer properties that must take place when the explosive melts. The experimental arrangement is shown in Fig. 8. Before firing the thin-walled cylindrical capsule containing the pressed or cast explosive is suspended above the Dural heating block as shown. When the heating block has

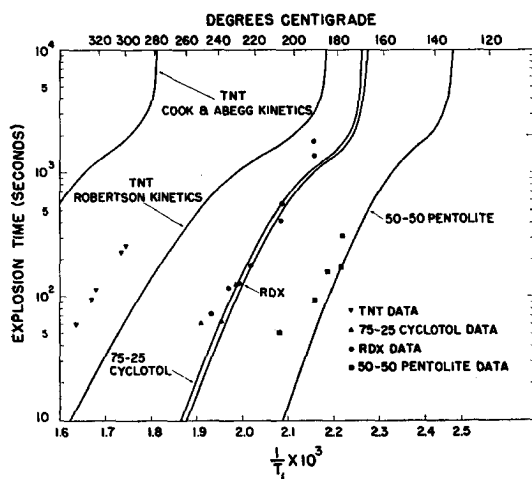


FIG. 7. Comparison of experimental and calculated induction times for various explosives.

<sup>7</sup> Rogers, Yasuda, and Zinn, Anal. Chem. (submitted for publication).

<sup>8</sup> A. J. B. Robertson, Trans. Faraday Soc. 45, 85 (1949).

<sup>9</sup> A. J. B. Robertson, J. Soc. Chem. Ind. (London) 61, 221 (1948).

<sup>10</sup> A. J. B. Robertson, Trans. Faraday Soc. 44, 977 (1948).

<sup>11</sup> M. A. Cook and M. T. Abegg, Ind. Eng. Chem., 48, 1090-1095 (1956).

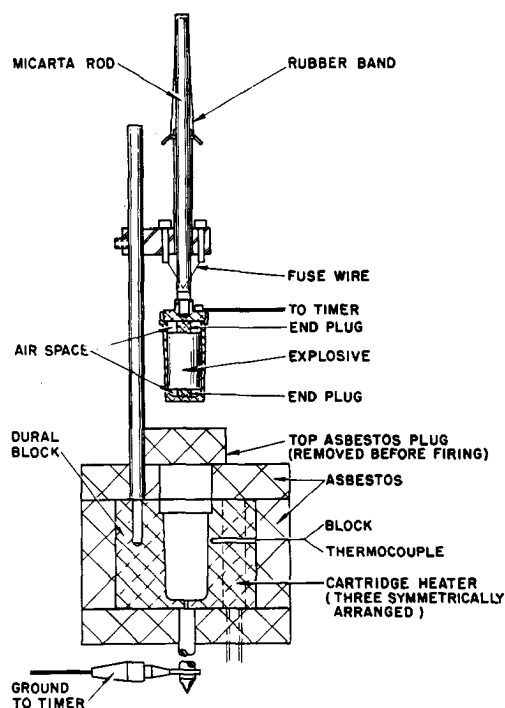


FIG. 8. The experimental arrangement.

attained the desired temperature the asbestos lid is removed and the fuse wire burned, causing the capsule to be propelled by the rubber band into the matching tapered hole in the block. The seating of the capsule completes an electrical circuit which starts a timer. The timer circuit is interrupted when explosion occurs, so that the explosion time is automatically recorded.

The temperature of the block is measured by a thermocouple, and remains essentially constant during a run. The explosive sample is fairly well insulated from the ends of the container, so that it is mathematically equivalent to an infinitely long cylinder. Heat transfer across the walls of the container is such that approximately 1 sec is required for the temperature at the inside

wall to increase by 90% of the difference between its initial value and the temperature of the block.

The explosion-time data for RDX, 75/25 cyclotol, 50/50 pentolite, and TNT are plotted in Fig. 7, along with the calculated curves for 1-in. cylinders. Except for TNT (where the kinetic data are in question) the agreement between theory and experiment is reasonably good.

#### ACKNOWLEDGMENTS

The authors wish to thank Mr. Edward James and Mr. Robert F. Warner for their help in designing equipment and supplying data. They are also indebted to Dr. L. C. Smith and Dr. W. Fickett for many helpful discussions.

## Single Crystal Tungstates for Resonance and Emission Studies

L. G. VAN UITERT AND R. R. SODEN

*Bell Telephone Laboratories, Incorporated, Murray Hill, New Jersey*

(Received May 27, 1959)

A number of single crystal tungstates have been prepared for paramagnetic resonance and emission studies. Compositions such as monoclinic  $\text{MgWO}_4$ ,  $\text{ZnWO}_4$ ,  $\text{CdWO}_4$ , and tetragonal  $\text{CaWO}_4$ ,  $\text{SrWO}_4$ , and  $\text{BaWO}_4$  containing paramagnetic ions of the transition and rare earth series have been prepared. They were grown by dissolving the constituent oxides into an equimolar mixture of  $\text{Na}_2\text{WO}_4$  and  $\text{WO}_3$  at 1100 to 1250°C and cooling at 2 to 3°C per hour to 700°C.

These crystals offer the advantages of one environment for the paramagnetic ions present, freedom from strain (hardness equal to that of iron), absence of random ordering effects, minimal effects from nuclear magnetic moments, and chemical stability. Large zero field splitting are observed in the monoclinic crystals, making them of interest for studies at high microwave frequencies. The tetragonal compositions are promising at the lower microwave frequencies and have shown very narrow resonance lines. Line widths as low as 1.5 Mc have been obtained in  $\text{CaWO}_4\text{:Mn}$ .

$\text{Na}_{0.5}\text{Y}_{0.5}\text{WO}_4$  crystals, which have the scheelite structure, were also grown. Random ordering effects of monovalent sodium and trivalent yttrium, however, result in a nonhomogeneous electrostatic environment throughout the crystals and hence cause broad paramagnetic resonance lines.

#### INTRODUCTION

THE divalent metal ion tungstates have been of interest for their luminescent properties for some time.<sup>1</sup> They also provide a number of outstanding host lattices for paramagnetic ions for resonance studies. Two classes of tungstate crystals are of particular interest: the monoclinic compounds  $\text{MgWO}_4$ ,  $\text{ZnWO}_4$ , and  $\text{CdWO}_4$ , which are isomorphous with  $\text{MnWO}_4$ ,  $\text{FeWO}_4$ ,  $\text{CoWO}_4$ ,  $\text{NiWO}_4$ , and  $\text{CuWO}_4$ ; and the tetragonal compounds  $\text{CaWO}_4$  (scheelite),  $\text{SrWO}_4$ ,  $\text{BaWO}_4$ , and  $\text{PbWO}_4$ , which are isomorphous with  $\text{Na}_{0.5}\text{R}_{0.5}\text{WO}_4$  where R is yttrium, lanthanum, and the rare earths in their trivalent states.

In the past the monoclinic crystals mentioned above have been grown by crystallization from a sodium chloride melt.<sup>2</sup> Only small crystals have been obtained

by this procedure, since the solubilities of these compounds are quite low in sodium chloride. The maximum furnace temperature that may be used with this solvent is limited by the vaporization of the NaCl and of the additives such as  $\text{NiCl}_2$  and  $\text{CoCl}_2$  and by the attack of the container by chloride ions.

Others<sup>3</sup> have grown sodium lanthanum tungstates and related rare earth crystals from  $\text{Na}_2\text{WO}_4$  with comparable success. Calcium tungstate has been grown by the above methods and also as large crystals by the Bridgeman technique.<sup>4</sup>

#### CRYSTAL GROWTH

$\text{Na}_2\text{WO}_4$  was studied as a possible solvent for growing divalent metal tungstate crystals. It was found that this compound offers considerable advantage over NaCl

<sup>1</sup> F. A. Kröger, *Some Aspects of the Luminescence of Solids* (Elsevier Publishing Company, Inc., New York, 1948).

<sup>2</sup> A. Geuther and E. Forsburg; *Ann. Chem. Liebigs* **120**, 270 (1861).

<sup>3</sup> L. G. Sillen and A. L. Nylander, *Arkiv Kemi Mineral Geol.* **17A**, No. 4 (1943).

<sup>4</sup> Zerfoss, Johnson, and Imbers, *Phys. Rev.* **75**, 320 (1949).